An analytical approach for drawing the 2D field profile of a finite-width electric dipole with shims using conformal mapping

M. J. Basso[1]

[1] *Beam Physics Group, TRIUMF, 4004 Wesbrook Mall, Vancouver, British Columbia V6T 2A3, Canada*

August 18, 2016

Abstract

Conformal mapping is used to derive an analytical solution for the two dimensional (2D) field profile of a finite-width electric dipole with rectangular shims. The solution is implemented in *Mathematica* for varying pole dimensions. Its results are compared to those calculated using *Opera-2D* and are found to be in good agreement for shim heights up to ∼10% the gap half-width. The potential for optimizing shim dimensions for electric dipoles and electromagnets using this solution is discussed.

1 Introduction and Theory

Conformal mapping is a transformation of one complex domain $\mathcal{T}$ to another complex domain $\mathcal{Z}$ that preserves local angles and for which an inverse mapping always exists [1, 2]. A conformal function is defined as a function which is single-valued and holomorphic with a nonzero first derivative over the complex domain of interest [1]. Conformal mapping is particularly useful in solving electrostatic and magnetostatic problems where solutions to Laplace's equation in a domain with a complicated geometry may be achieved by first solving Laplace's equation in a domain with a simpler geometry and then by finding the appropriate conformal mapping between the two domains. If we write the position z of a point in a 2D complex domain $\mathcal{Z}$ as:

$$z = x + iy\,, \tag{1}$$

where x and y denote positions along the two coordinate axes and i is the imaginary unit, then we may similarly write the complex electric field E as:

$$E = E_x + iE_y\,, \tag{2}$$

where E_x and E_y are the x- and y-components of the electric field, respectively [1]. This electric field may be calculated from the complex potential ϕ as:

$$E = -\overline{\left(\frac{\partial\phi}{\partial z}\right)}\,, \tag{3}$$

where the overbar denotes complex conjugation [1]. In this document, it is our objective to use conformal mapping to analytically determine the 2D field profile of a rectangular electric dipole of a fixed width with shims. Shims are strips of metal attached to the end of each pole and are added to improve the field uniformity. While they typically have complicated geometries, we will consider only rectangular shims of a particular width and height for the purposes of this document.

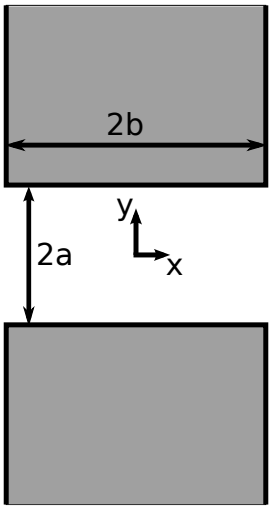

Figure 1: A drawing of the x-y plane showing the geometry of the finite-width dipole from Davy's conformal map [1, 3]. The poles have a width of $2b$ and a separation of $2a$. The origin is taken to be at the center of the dipole.

An analytical conformal map already exists for a finite-width dipole without shims of gap width $2a$ and pole width $2b$, derived by Davy in 1944 using the Schwartz-Christoffel transformation[1] [1, 3]. The geometry of this dipole is shown in Fig. 1. Davy's conformal map transforms from $\mathcal{T}$ with $t = r + is$ to $\mathcal{Z}$ with $z = x + iy$ and maps the positive s axis to the entire x axis and the positive and negative r axes to the surfaces of the bottom and the top pole, respectively [3]. The conformal map as function of u, where u is an intermediate variable defined by $\mathrm{sn}(u,k) = t^{-1}$, is given by:

$$z(u) = \frac{ai}{2E(k) - k'^2 K(k)} \left(k'^2 u - 2E(\mathrm{am}(u,k),k) - \frac{\mathrm{cn}(u,k)\,\mathrm{dn}(u,k)}{\mathrm{sn}(u,k)} \right) + b\,, \tag{4}$$

where $K(k)$ and $E(k)$ are the complete elliptic integrals of the first and second kind, respectively, $\mathrm{am}(u,k)$ is the Jacobi amplitude function, and $\mathrm{sn}(u,k)$, $\mathrm{cn}(u,k)$, and $\mathrm{dn}(u,k)$ are sine, cosine, and delta amplitude functions, respectively, also called the Jacobi elliptic functions[2] [1, 3]. An elliptic integral of second kind E with two arguments is taken to be an incomplete elliptic integral. All of these functions have a modulus k which solves:

$$\frac{k'^2 K(k') - 2K(k') + 2E(k')}{2\left(k'^2 K(k) - 2E(k)\right)} = \frac{b}{a}\,, \tag{5}$$

where $0 < k < 1$ and $k' = \sqrt{1 - k^2}$ is the complementary modulus [1, 3]. The Jacobi amplitude function $\mathrm{am}(u,k) = \arcsin(\mathrm{sn}(u,k))$ is related to u by $F(\mathrm{am}(u,k),k) = u$, where F is the incomplete elliptic integral of the first kind [4]. Given that $\mathrm{sn}(u,k) = t^{-1}$, we may write u as:

$$u = F(\arcsin(t^{-1}),k)\,. \tag{6}$$

[1]The details of the Schwartz-Christoffel transformation are unimportant but are explained in Ref. [1] for the interested reader.

[2]Eq. 4 differs from Eq. 12 of Ref. [3] in that there is an $\mathrm{am}(u,k)$ as the argument of the incomplete elliptic intergal of the second kind instead of a u. The author believes Walstrom made a mistake as evaluating $z(u)$ for the u that pertains to $t = k$ and $t = 1$ where $\mathrm{sn}(u,k) = t^{-1}$ does not yield $z = -b + ia$ and $z = b + ia$ as it should when there is $E(u,k)$ instead of $E(\mathrm{am}(u,k),k)$, according to that same paper. The replacement gives the correct result. Additionally, in the last paragraph of page 3 of Ref. [3], the expanded form of $E(u)$ should be multiplied by a -1.

Additionally, $\mathrm{cn}(u,k) = \sqrt{1-\mathrm{sn}(u,k)^2}$ and $\mathrm{dn}(u,k) = \sqrt{1-k^2\,\mathrm{sn}(u,k)^2}$ [5]. As a result, we may write:

$$\frac{\mathrm{cn}(u,k)\,\mathrm{dn}(u,k)}{\mathrm{sn}(u,k)} = \frac{\sqrt{t^2-1}\sqrt{t^2-k^2}}{t}\,, \tag{7}$$

and substituting Eqs. 6 and 7 into Eq. 4 yields:

$$z(t) = \frac{ia}{2E(k)-k'^2K(k)}\left(k'^2F(\arcsin(t^{-1}),k) - 2E(\arcsin(t^{-1}),k) - \frac{\sqrt{t^2-1}\sqrt{t^2-k^2}}{t}\right) + b\,, \tag{8}$$

which is an expression for Davy's conformal map in terms of t [1].

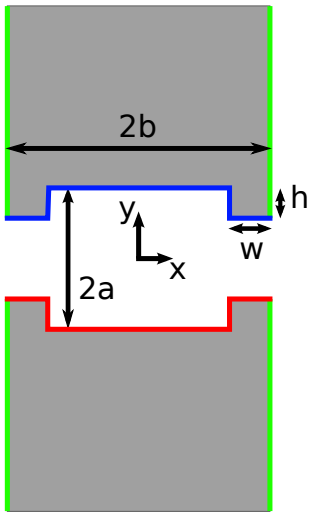

Figure 2: A drawing of the x-y plane showing the geometry of the finite-width dipole with rectangular shims on the ends of each pole. The poles have a width of $2b$ and a separation of $2a$ The shims have a height of h and a width of w; the relative width and height of the shims are exaggerated for clarity. The red surface is held at a potential of $+V_0$, the blue surface is held at a potential of $-V_0$, and the green surfaces are grounded. The origin is taken to be at the center of the dipole.

The geometry of our dipole with shims is shown in Fig. 2. It is identical to the dipole shown Fig. 1 with the exception of the rectangular shims of height h and width w attached to the ends of each pole. To excite our dipole, we set the potential along the surface of the lower pole's tip to $+V_0$, the potential along the surface of the upper pole's tip to $-V_0$, and we ground the sides of each pole, as shown in Fig. 2. Now, we make an approximation: our problem can be simplified by approximating our finite-width dipole with shims as a finite-width dipole without shims of the same pole width but with a pole gap of $2(a-h)$ instead of $2a$. This approximation is valid for $h/a \ll 1$. With this approximation, Davy's conformal map becomes:

$$z(t) = \frac{i(a-h)}{2E(k)-k'^2K(k)}\left(k'^2F(\arcsin(t^{-1}),k) - 2E(\arcsin(t^{-1}),k) - \frac{\sqrt{t^2-1}\sqrt{t^2-k^2}}{t}\right) + b\,, \tag{9}$$

with a modulus k given by:

$$\frac{k'^2K(k') - 2K(k') + 2E(k')}{2\left(k'^2K(k) - 2E(k)\right)} = \frac{b}{a-h}\,, \tag{10}$$

where we have replaced the a's in Eqs. 5 and 8 with $(a-h)$'s. In making this approximation, we also need to adjust the potential along the surface of the pole in $\mathcal{Z}$ as shown in Fig. 3. The lower pole surface between $z=-(b-w)-i(a-h)$ and $z=b-w-i(a-h)$ is adjusted to the natural guess of $+(1-h/a)V_0$, which is valid for $h/a \ll 1$. In a similar way, the upper pole surface between $z=-(b-w)+i(a-h)$ and $z=b-w+i(a-h)$ is adjusted to the natural guess of $-(1-h/a)V_0$. The remaining surfaces have the same potentials as those in Fig. 2.

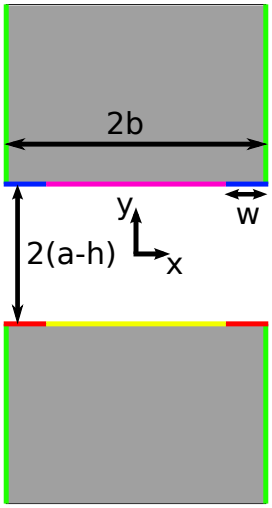

Figure 3: A drawing of the x-y plane showing the geometry of the finite-width dipole obtained through applying our $h/a \ll 1$ approximation to the dipole geometry shown in Fig. 2. The red surfaces are held at a potential of $+V_0$, the yellow surface us held at a potential of $+(1-h/a)V_0$, the blue surfaces are held at a potential of $-V_0$, the purple surface is held at a potential of $-(1-h/a)V_0$, and the green surfaces are grounded. The red and blue surfaces have the same length, and the yellow and purple surfaces have the same length. The origin is taken to be at the center of the dipole.

With our conformal map determined, we only need to find the potential for $t=r+is$ with $s>0$ in $\mathcal{T}$ corresponding to arrangement of potentials in Fig. 3. If we let $t=r_1$, $t=r_2$, $t=-r_1$, and $t=-r_2$ correspond to $z=b-w-i(a-h)$, $z=-(b-w)-i(a-h)$, $z=b-w+i(a-h)$, and $z=-(b-w)-i(a-h)$, respectively, then the arrangement of potentials along the r-axis in $\mathcal{T}$ is as shown in Fig. 4.

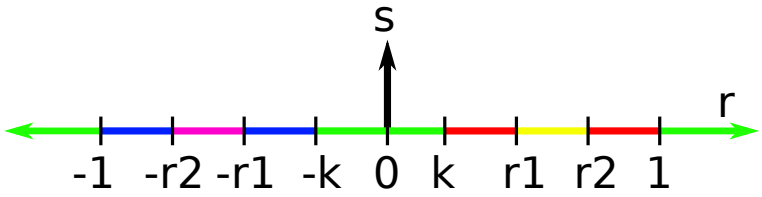

Figure 4: A drawing of the r-s plane showing the arrangement of potentials corresponding to Fig. 3. The red surfaces are held at a potential of $+V_0$, the yellow surface is held at a potential of $+(1-h/a)V_0$, the blue surfaces are held at a potential of $-V_0$, the purple surface is held at a potential of $-(1-h/a)V_0$, and the green surfaces are grounded. The relative lengths are not to scale.

Solving for the potential for $s>0$ in $\mathcal{T}$ is identical to solving the N-value Dirichlet problem in the upper-half plane, whose solution is given by a superposition appropriately-shifted and appropriately-scaled arctangent functions [6]. The potential for $s>0$ can be shown to equal:

$$\phi = \frac{2V_0}{\pi}\left(\arctan\left(\frac{s}{r-1}\right) - \arctan\left(\frac{s}{r-r_2}\right) + \arctan\left(\frac{s}{r-r_1}\right) - \arctan\left(\frac{s}{r-k}\right) - \arctan\left(\frac{s}{r+k}\right) + \arctan\left(\frac{s}{r+r_1}\right) - \arctan\left(\frac{s}{r+r_2}\right) + \arctan\left(\frac{s}{r+1}\right)\right) + \frac{2V_0}{\pi}\left(1-\frac{h}{a}\right)\left(\arctan\left(\frac{s}{r-r_2}\right) - \arctan\left(\frac{s}{r-r_1}\right) - \arctan\left(\frac{s}{r+r_1}\right) + \arctan\left(\frac{s}{r+r_2}\right)\right). \tag{11}$$

To solve for r_1 and r_2, we note that the surface along the lower pole between $z = -b - i(a-h)$ and $z = b - i(a-h)$ is mapped to by $t = r$ for $k < t < 1$ [1, 3]. With this in mind, we define a function which maps to this lower surface $C_3(r)$ as:

$$C_3(r) \equiv z(t)\Big|_{t=r,k<r<1}, \tag{12}$$

and substituting Eq. 9 into Eq. 12 and simplifying yields:

$$C_3(r) = \frac{-(a-h)}{2E(k) - k'^2K(k)}\left((1+k^2)F\left(\arcsin\left(\sqrt{\frac{1-t^2}{1-k^2}}\right), k'\right) - 2E\left(\arcsin\left(\sqrt{\frac{1-t^2}{1-k^2}}\right), k'\right) + \frac{\sqrt{1-t^2}\sqrt{t^2-k^2}}{t}\right) + b - i(a-h), \tag{13}$$

for $k < r < 1$, as derived by Schweitzer[3] in Ref. [1]. Now one may solve for r_1 and r_2 by solving $C_3(r_1) = -(b-w) - i(a-h)$ and $C_3(r_2) = b - w - i(a-h)$[4], respectively.

To find the electric field in $\mathcal{Z}$, we apply the chain rule to Eq. 3:

$$E = -\overline{\left(\frac{\partial\phi}{\partial z}\right)} = -\overline{\left(\left(\frac{\partial\phi}{\partial t}\right)\left(\frac{\partial z}{\partial t}\right)^{-1}\right)}. \tag{14}$$

The partial derivative of ϕ with respect to t may be written as a sum of partial derivatives of ϕ with respect to r and s as:

$$\frac{\partial\phi}{\partial t} = \frac{1}{2}\left(\frac{\partial\phi}{\partial r} - i\frac{\partial\phi}{\partial s}\right), \tag{15}$$

which is referred to as a Wirtinger derivative [7]. Inserting Eq. 15 in Eq. 14 yields:

$$E = -\overline{\left(\frac{1}{2}\left(\frac{\partial\phi}{\partial r} - i\frac{\partial\phi}{\partial s}\right)\left(\frac{\partial z}{\partial t}\right)^{-1}\right)}. \tag{16}$$

We may evaluate our field along the x-axis in $\mathcal{Z}$ by setting $t = is$ for $s > 0$ in Eq. 16. Additionally, we recognize that $E_x = 0$ along the x-axis in $\mathcal{Z}$ by symmetry and so E is purely imaginary. To extract E_y, we take the imaginary part of Eq. 16. The y-component of the electric field along the x-axis as function of s is therefore:

$$E_y \equiv E_y\Big|_{y=0} = \Im\left\{\left[-\overline{\left(\frac{1}{2}\left(\frac{\partial\phi}{\partial r} - i\frac{\partial\phi}{\partial s}\right)\left(\frac{\partial z}{\partial t}\right)^{-1}\right)}\right]\Big|_{t=is}\right\}. \tag{17}$$

[3]It should be noted that Schweitzer appears to define his t as the inverse of the t presented in the equations of this document. For an example, see from Eq. 35 in his thesis. In using his derived $C_3(r)$, we have inverted the t's as appropriate and set them equal to r.

[4]The author notes that r_1 and accordingly k are typically very small. This fact may make them difficult to solve for. Applying a log transform to r_1 and k could help in this endeavour but has yet to be rigorously tested.

We insert Eqs. 9 and 11 into Eq. 17 and simplify the resulting expression to yield:

$$E_y(s) = \frac{2V_0\left(2E(k) - k'^2K(k)\right)}{\pi(a-h)} \frac{s^3}{\sqrt{s^2+1}\sqrt{s^2+k^2}} \left(\frac{1}{s^2+k^2} - \frac{1}{s^2+1} + \frac{h}{a}\left(\frac{1}{s^2+r_2^2} - \frac{1}{s^2+r_1^2}\right)\right), \quad (18)$$

for $s > 0$ as our expression for field profile of an electric dipole along the x-axis with a gap width of $2a$, a pole width of $2b$, a shim height of h, and a shim width of w with $\pm V_0$ on the surfaces of each of the pole tips, parametrized in terms of s. To complete our solution, we solve for x parametrized in terms of s for $y = 0$ by evaluating $z(t)$ for $t = is$ where $s > 0$, a purely real result:

$$x(s) \equiv x(s)\Big|_{y=0} = z(t)\Big|_{t=is, s>0}. \quad (19)$$

We insert Eq. 9 into Eq. 19 and simplify the resulting expression to yield:

$$x(s) = \frac{a-h}{2E(k) - k'^2K(k)} \left(2E(\arctan(s^{-1}), k') - (1+k^2)F(\arctan(s^{-1}), k') - \frac{2}{s}\sqrt{\frac{s^2+k^2}{s^2+1}} + \frac{\sqrt{s^2+k^2}\sqrt{s^2+1}}{s}\right) + b, \quad (20)$$

for $s > 0$, as derived by Walstrom[5] in Ref. [3], and this completes our analytical solution. Eqs. 18 and 20 represent a set of parametric equations implicitly defining E_y as a function of x.

2 Implementation

Our analytical solution was implemented in Wolfram's *Mathematica*. The *Mathematica* notebook used is included in Appendix A. To find the field profile of dipole with a given set of dimensions, the modulus k was first determined by solving Eq. 10 numerically using *Mathematica*'s **FindRoot[ ]** command. Using Eq. 13, $C_3(r_1) = -(b-w) - i(a-h)$ and $C_3(r_2) = b - w - i(a-h)$ were similarly solved for r_1 and r_2, respectively. It was found that the **ParametricPlot[ ]** command did not correctly plot $E_y(s)$ as a function of $x(s)$. Instead, Eqs. 18 and 20 were each evaluated for a logarithmically-distributed vector of s values and the resulting set of points were then plotted to draw the field profile. This procedure was performed for three dipoles, each with different dimensions. Cobham's *Opera-2D* was used to numerically solve for the field profiles of three dipoles with the same set of dimensions in order to provide a standard to which the results of our analytical solution may be compared. The length of poles in the *Opera-2D* model were made many times larger than the pole gap width as the poles are assumed to be infinitely long within Davy's conformal map [1]. Additionally, our solution pertains to the high-conductivity limit of the poles and so the material composing the poles in the *Opera* simulation was specified to have a conductivity of $\sim 10^8$ S/m. The edges of the background bounding our *Opera* model were made far from the center of the dipole to ensure that edge effects did not interfere with the calculated field profiles through the dipoles.

3 Results and Discussion

The results of our analytical solution for the three different dipoles considered and the *Opera-2D* results for the corresponding dipoles are shown in Figs. 5, 6, and 7.

[5]Incidentally, Walstrom correctly derived Eq. 20 from $z(t)$ even though he used a $E(u)$ instead of a $E(\mathrm{am}(u,k),k)$

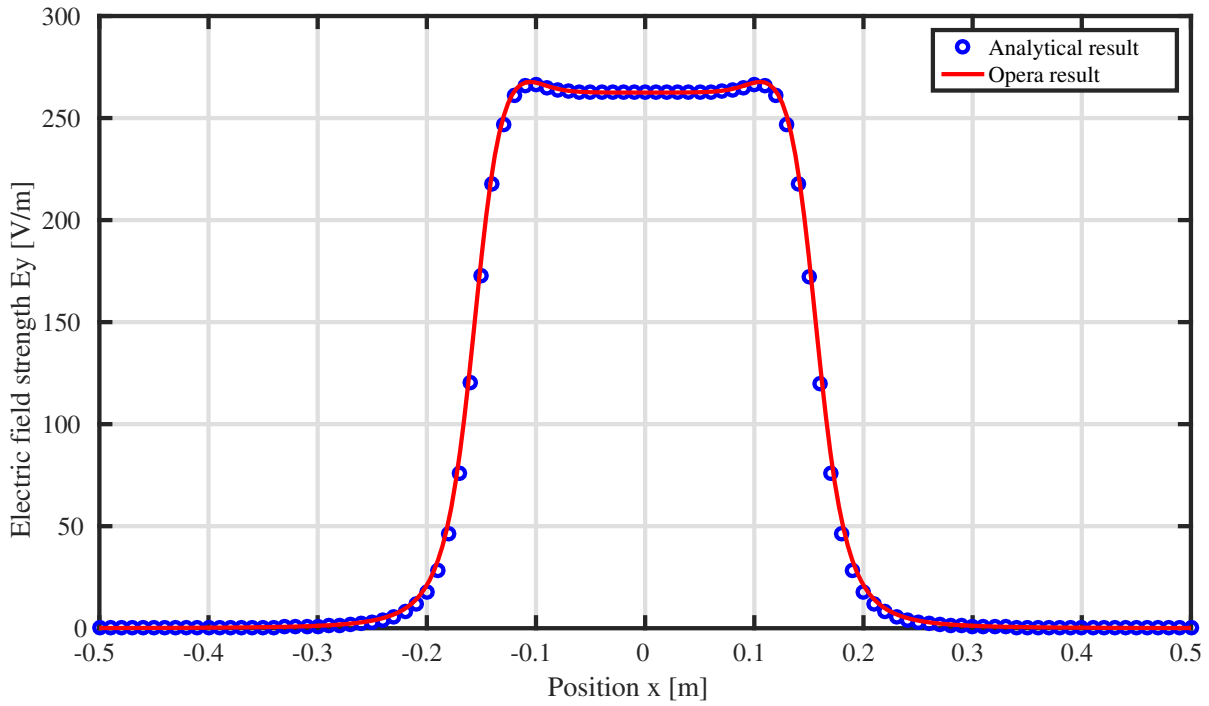

Figure 5: The analytical result and the *Opera-2D* result for the field profile of an electric dipole with $a = 38.1$ mm, $b = 152.4$ mm, $h = 1.905$ mm, $w = 50.0$ mm, and $V_0 = 20.0$ V.

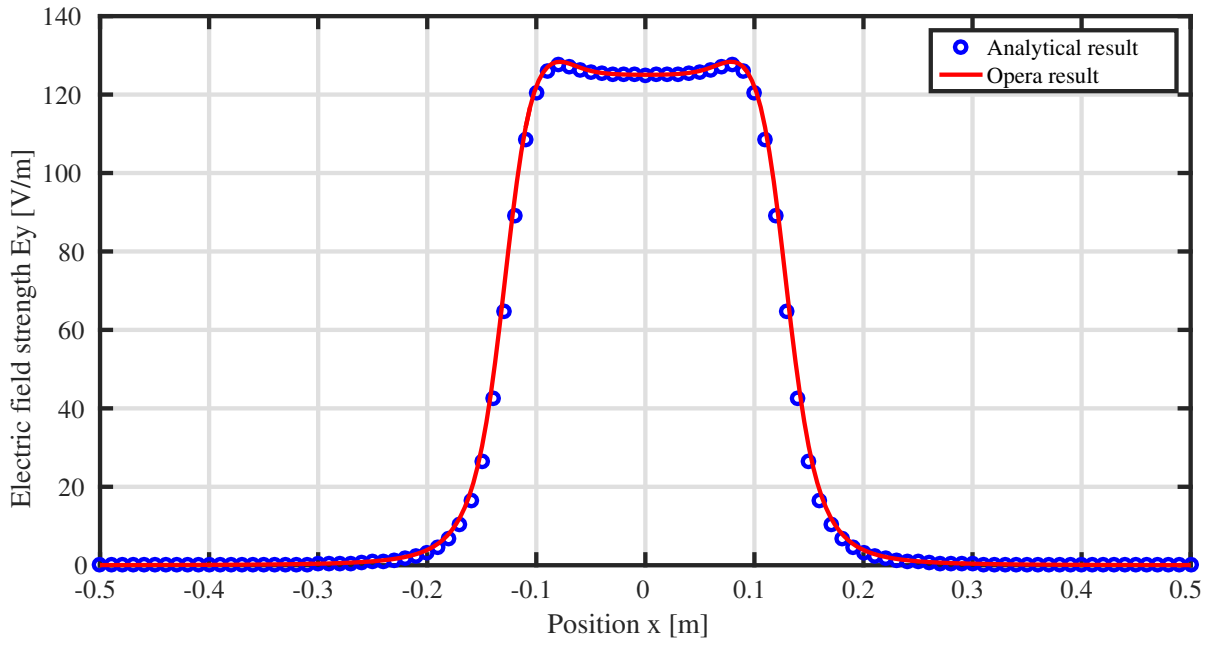

Figure 6: The analytical result and the *Opera-2D* result for the field profile of an electric dipole with $a = 40.0$ mm, $b = 125.0$ mm, $h = 2.5$ mm, $w = 50.0$ mm, and $V_0 = 10.0$ V.

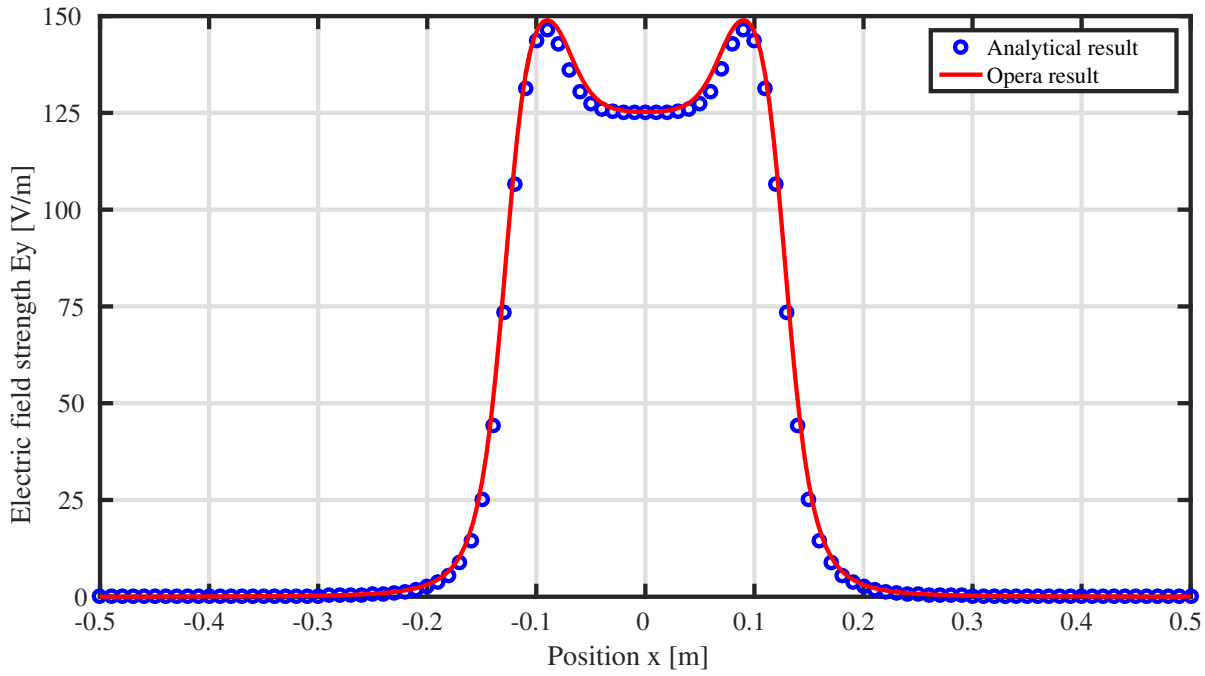

Figure 7: The analytical result and the *Opera-2D* result for the field profile of an electric dipole with $a = 40.0$ mm, $b = 125.0$ mm, $h = 8.0$ mm, $w = 50.0$ mm, and $V_0 = 10.0$ V.

By visual assessment, the agreement between the analytical solution and *Opera-2D* results is very good for each of the dipoles considered. In Figs. 5 and 6, the plotted data sets nearly overlap perfectly with one another, but this was to be expected. In deriving our solution, we assumed the shim height h was small relative to the gap half-width a. This approximation is valid in Figs. 5 and 6 where $h/a = 0.05$ and 0.0625, respectively. In Fig. 7, the analytical solution begins to deviate from the *Opera-2D* results around the "ears" of the field profile. For this last dipole, $h/a = 0.1$ and so it is possible that this dipole has dimensions which are out of the range of validity for our solution. However, the analytical solution does agree with most data points obtained from the *Opera-2D* simulation. With this in mind, we conclude that our analytical solution works best for $h/a \lesssim 0.1$.

4 Summary and Applications

In this document, we have presented an analytical solution for the field profile of a finite-width electric dipole with shims. This result would have previously been obtainable only through numerically means. The analytical solution was used to solve for the field profiles of three different dipoles. These results were compared to field profiles obtained using *Opera-2D* and found to be in good agreement for shim heights up to ∼10% of the pole gap half-width. No approximation was made concerning the shim width and so the shims may be as wide as the pole half-width b. For future work, it would be useful to explore the accuracy of the model for a wider range of pole and shim dimensions as well as to explore the statistical significance of the agreement between the analytical solution and *Opera*. It is also possible to generalize our solution for the case where the potential along the surface of the pole tip also extends along the sides of the pole for some distance d above the pole tip at $y = \pm a$, but this would add two additional constants to be solved for: r_3 and r_4 where $z(r_3) = -b - (a + d)i$ and $z(r_4) = -b - (a + d)i$.

Besides enabling one to quickly produce field profiles, our analytical solution opens the possibility of analytically optimizing shim dimensions such that field uniformity through the dipole is maximized. Opti-

mization packages in programs like *Opera* would typically be used to numerically optimize shim dimensions but are not readily available to everyone. Even with *Opera* optimization packages a person may not have an initial guess of what the approximate optimal shims are. One should, in principle, be able to use our analytical solution to find a particular solution for the optimal dimensions of rectangular shims within the framework of their specified optimization condition. Again, shims typically have complicated shapes, but the dimensions provided by optimizing our solution would be a starting point for these shapes. We have identified two possible optimization conditions. The first optimization condition specifies the optimal shims as those that maximize field flatness at the centre of the dipole for a fixed gap width $2a$ and a fixed pole width $2b$. To maximize the field flatness, the optimal shims must set the second and fourth derivatives of the field with respect to x to zero at the center of the dipole, as the first and third derivatives are already zero at that position. We suppose that $s = s_0$ is defined by $x(s_0) = 0$. The equations used to determine s_0, k, r_1, and r_2, Eqs. 20, 10, and 13, all depend on at least h and sometimes w. Eq. 18, which is used to calculate d^2E_y/dx^2 and d^4E_y/dx^4, also depends on h. As a result, we have to solve a set of six coupled, non-linear equations for h, w, k, s_0, r_1, and r_2, which are given by:

$$\left\{ \begin{array}{rcl} x(s=s_0,h,k) & = & 0 \\ C_3(r=r_1,h,k) & = & -(b-w)-i(a-h) \\ C_3(r=r_2,h,k) & = & b-w-i(a-h) \\ \frac{b}{a-h} & = & \frac{k'^2K(k')-2K(k')+2E(k')}{2(k'^2K(k)-2E(k))} \\ \left.\frac{\partial^2 E_y}{\partial x^2}\right|_{s=s_0,r_1,r_2,h,k} & = & 0 \\ \left.\frac{\partial^4 E_y}{\partial x^4}\right|_{s=s_0,r_1,r_2,h,k} & = & 0 \end{array} \right\}, \tag{21}$$

with search restrictions $0 < w < b$, $0 < a < h$, $k < r_1 < r_2 < 1$, $0 < k < 1$, and $0 < s_0$. The derivatives of Ey with respect to x are calculated using Eqs. 18 and 20 in the usual way for parametric equations:

$$\frac{\partial^2 E_y}{\partial x^2} = \partial_s[\partial_s Ey(s)/\partial_s x(s)]/\partial_s x(s)\,, \tag{22}$$

$$\frac{\partial^4 E_y}{\partial x^4} = \partial_s\left[\partial_s \frac{\partial^2 E_y}{\partial x^2}\Big/\partial_s x(s)\right]\Big/\partial_s x(s)\,, \tag{23}$$

where ∂_s denotes differentiation with respect to s [3]. The expression for $\partial_s x(s)$ is relatively simple:

$$\partial_s x(s) \equiv \frac{\partial x}{\partial s} = \frac{a-h}{2E(k)-k'^2K(k)}\frac{\sqrt{s^2+k^2}\sqrt{s^2+1}}{s^2}\,, \tag{24}$$

for $s > 0$. Now, the equations in Eq. 21 must be solved accurately as the derivatives of E_y are already relatively close to zero for poles where $b/(a-h) \gtrsim 3$. Solving these equations is made somewhat simpler by assuming $k \ll 1$, which is valid for $b/(a-h) > 2$ [3]. This approximation eliminates the fourth equation in Eq. 21 and simplifies the remaining equations by taking the limit $k \to 0$. However, the system is still quite complicated in this limit[6].

Alternatively, our second optimization condition identifies the optimal shims as those which result in a field value of $E_{y,1}$ at position $x = x_1 > 0$ which satisfies the specified field falloff $|(E_{y,1} - E_{y,0})/E_{y,0}| < T$, where $E_{y,0}$ is the field value at $x = 0$ and T is the specified tolerance. The gap width and the pole width are also specified. Ideally, the pole width would be as small as possible, but this would add an additional layer of numerical optimization. It is unclear to the author how to account for this final requirement. Future work will examine this may be achieved.

Finally, we may also use our solution to optimize the shims dimensions for a finite-width magnetic dipole. This situation is analogous to the electric dipole we have considered if one imagines layering magnetic potential onto the surface of the poles instead of electric potential. Additionally, the optimal shim dimensions

[6]The author has attempted to solve the system of equations in this limit by using *Mathematica*'s **FindRoot**[ ] command as well as by using simulated annealing in FORTRAN, but has had no present success.

found for an electric dipole should match those found for the corresponding magnetic dipole as we expect the field expressions in each case to be scalar multiples of one another. Testing the ability of our model to predict the field profiles of magnetic dipoles up to a scaling factor is another area to be explored by future work.

5 Acknowledgements

The author would like to thank Paul Jung, Thomas Planche, and Yi-Nong Rao for their assistance in deriving the solution presented in this document as well as in formulating the problem for the optimization of shim dimensions. The author would also like to thank TRIUMF for his use of *Mathematica* and *Opera-2D*.

References

[1] G. Schweitzer, "Quickly Available Graphics of Static, Electromagnetic Field Distributions Given by Conformal Maps Using *Mathematica*," Diploma thesis, Inst. Theor. Phys., Tech. Univ. Graz, Styria, Austria, 1995.

[2] E. W. Weisstein. (2016). *Conformal Mapping* [Online]. Available: `http://www.mathworld.wolfram.com/ConformalMapping.html` [Accessed: July 2016].

[3] P. L. Walstrom, "Dipole-magnet field models based on a conformal map," *Phys. Rev. ST Accel. Beams*, vol. 15, no. 10, pp. 102401-1–7, Oct. 2012.

[4] E. W. Weisstein. (2016). *Jacobi Amplitude* [Online]. Available: `http://www.mathworld.wolfram.com/JacobiAmplitude.html` [Accessed: July 2016].

[5] E. W. Weisstein. (2016). *Jacobi Elliptic Functions* [Online]. Available: `http://www.mathworld.wolfram.com/JacobiEllipticFunctions.html` [Accessed: July 2016].

[6] J. H. Mathews and R. W. Howell. (2012). *Module for Laplace's Equation and Dirichlet Problem* [Online]. Available: `http://mathfaculty.fullerton.edu/mathews/c2003/DirichletProblemMod.html` [Accessed: July 2016].

[7] R. Hunger, "An Introduction to Complex Differentials and Complex Differentiability," Assoc. Inst. Signal Process., Tech. Univ. Munich, Germany, Tech. Rep. TUM-LNS-TR-07-06, p. 9, 2007.

Appendices

A *Mathematica* Notebook Used for Drawing Field Profiles

The following *Mathematica* notebook was used to draw the field profiles presented in this document. For a given a, b, h, w, and V_0, the profiles of the electric field and its first, second, third, and fourth derivatives are outputted. The solution presented in the following notebook pertains to the dipole whose field data is shown in Fig. 5. The notebook has been annotated for clarity.

In[1]:=
```
Clear["Global`*"];

(*The parameters defining the dipole are entered below. xmin and xmax refer to the
 minimum and maximum values of x over the domain to be considered, respectively.*)

a = 381 / 10 000;
b = 1524 / 10 000;
w = 500 / 10 000;
h = 1905 / 1 000 000;
V0 = 10;
xmin = -0.5;
xmax = 0.5;

(*k, r1, and r2 are solved for using the FindRoot[ ] command. smin
 and smax are the s values corresponding to xmin and xmax, respectively,
and are also solved for using FindRoot[ ]. The initial search values for FindRoot[ ]
 may need to be updated for new dipole parameters to ensure accurate results.*)

f[k_] = (2 * EllipticE[1 - k^2] - (1 + k^2) * EllipticK[1 - k^2]) / 2 /
    (EllipticK[k^2] * (1 - k^2) - 2 * EllipticE[k^2]);
k = FindRoot[f[k] == b / (a - h), {k, 1*^-7}, WorkingPrecision → 10][[All, 2]][[1]]
C3[t_] = -(a - h) * ((1 + k^2) * EllipticF[ArcSin[Sqrt[(1 - t^2) / (1 - k^2)]], 1 - k^2] -
        2 * EllipticE[ArcSin[Sqrt[(1 - t^2) / (1 - k^2)]], 1 - k^2] +
        Sqrt[1 - t^2] * Sqrt[t^2 - k^2] / t) /
      (2 * EllipticE[k^2] - (1 - k^2) * EllipticK[k^2]) + b - I * (a - h);
r1 = FindRoot[C3[t] == w - b - I * (a - h), {t, 1*^-5, k, 1}, WorkingPrecision → 9][[
    All, 2]][[1]]
r2 = FindRoot[C3[t] == b - w - I * (a - h), {t, 0.01, k, 1}, WorkingPrecision → 9][[All, 2]][[
   1]]
x[s_] = (a - h) * (2 * EllipticE[ArcTan[1 / s], 1 - k^2] -
        (1 + k^2) * EllipticF[ArcTan[1 / s], 1 - k^2] -
        2 * Sqrt[s^2 + k^2] / Sqrt[s^2 + 1] / s + Sqrt[s^2 + 1] * Sqrt[s^2 + k^2] / s) /
      (2 * EllipticE[k^2] - (1 - k^2) * EllipticK[k^2]) + b;
smin = FindRoot[x[s] == xmin, {s, 1*^-8}][[All, 2]][[1]]
smax = FindRoot[x[s] == xmax, {s, 10}][[All, 2]][[1]]

(*Dx refers to the derivative of x with respect to s. Ey is defined. D1Ey, D2Ey, D3Ey,
D4Ey are the first, second, third, and fourth derivatives of Ey with respect to x,
respectively, and are calculated below in the typical way for parametric equations.*)

Dx[s_] = (a - h) / (2 * EllipticE[k^2] - (1 - k^2) * EllipticK[k^2]) *
    Sqrt[s^2 + k^2] * Sqrt[s^2 + 1] / s^2;
Ey[s_] = V0 * 2 / Pi * (2 * EllipticE[k^2] - (1 - k^2) * EllipticK[k^2]) / (a - h) *
    s^3 / Sqrt[s^2 + 1] / Sqrt[s^2 + k^2] *
    (1 / (s^2 + k^2) - 1 / (s^2 + 1) + h / a * (1 / (s^2 + r2^2) - 1 / (s^2 + r1^2)));
D1Ey[s_] = ∂s Ey[s] / Dx[s];
D2Ey[s_] = ∂s D1Ey[s] / Dx[s];
```

```
D3Ey[s_] = ∂s D2Ey[s] / Dx[s];
D4Ey[s_] = ∂s D3Ey[s] / Dx[s];
```

(*Ey, D1Ey, D2EY, D3Ey,
and D4Ey are evaluated for a logarithmically−distributed s vector between smin and smax using the Table[ ] command. Each of these are then plotted as a function of x, which has also been evaluated for the same s vector.*)

```
data1 =
  Table[{x[Exp[q]], Ey[Exp[q]]}, {q, Log[smin], Log[smax], Log[smax / smin] / 1000}];
data2 = Table[{x[Exp[q]], D1Ey[Exp[q]]},
   {q, Log[smin], Log[smax], Log[smax / smin] / 1000}];
data3 = Table[{x[Exp[q]], D2Ey[Exp[q]]},
   {q, Log[smin], Log[smax], Log[smax / smin] / 1000}];
data4 = Table[{x[Exp[q]], D3Ey[Exp[q]]},
   {q, Log[smin], Log[smax], Log[smax / smin] / 1000}];
data5 = Table[{x[Exp[q]], D4Ey[Exp[q]]},
   {q, Log[smin], Log[smax], Log[smax / smin] / 1000}];
plot1 = ListLinePlot[data1, PlotRange → {{xmin, xmax}, {Automatic, Automatic}},
  ImageSize → Large, Frame → True, GridLines → Automatic, AxesLabel → {x, Ey}]
plot2 = ListLinePlot[data2, PlotRange → {{xmin, xmax}, {Automatic, Automatic}},
  ImageSize → Large, Frame → True, GridLines → Automatic, AxesLabel → {x, D1Ey}]
plot3 = ListLinePlot[data3, PlotRange → {{xmin, xmax}, {Automatic, Automatic}},
  ImageSize → Large, Frame → True, GridLines → Automatic, AxesLabel → {x, D2Ey}]
plot4 = ListLinePlot[data4, PlotRange → {{xmin, xmax}, {Automatic, Automatic}},
  ImageSize → Large, Frame → True, GridLines → Automatic, AxesLabel → {x, D3Ey}]
plot5 = ListLinePlot[data5, PlotRange → {{xmin, xmax}, {Automatic, Automatic}},
  ImageSize → Large, Frame → True, GridLines → Automatic, AxesLabel → {x, D4Ey}]
```

Out[10]= $9.731738223 \times 10^{-7}$

Out[12]= 0.0000114654712

Out[13]= 0.0841639791

Out[15]= 6.43761×10^{-8}

Out[16]= 15.1183

Out[28]=

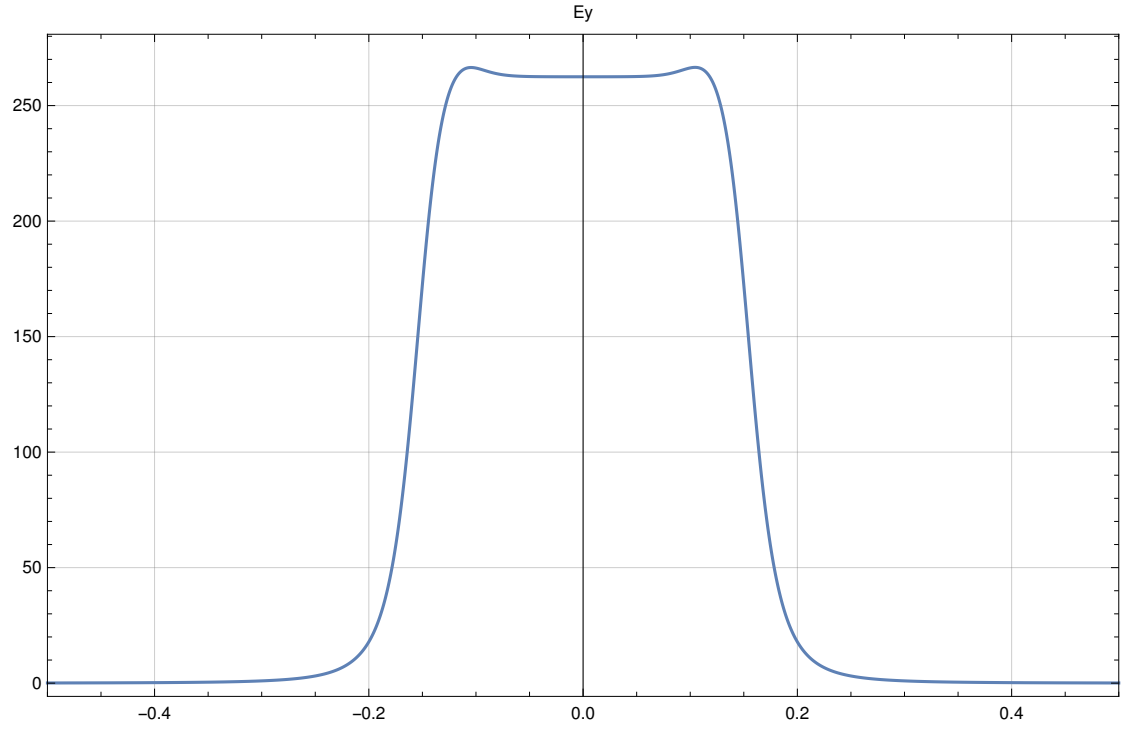

Out[29]=

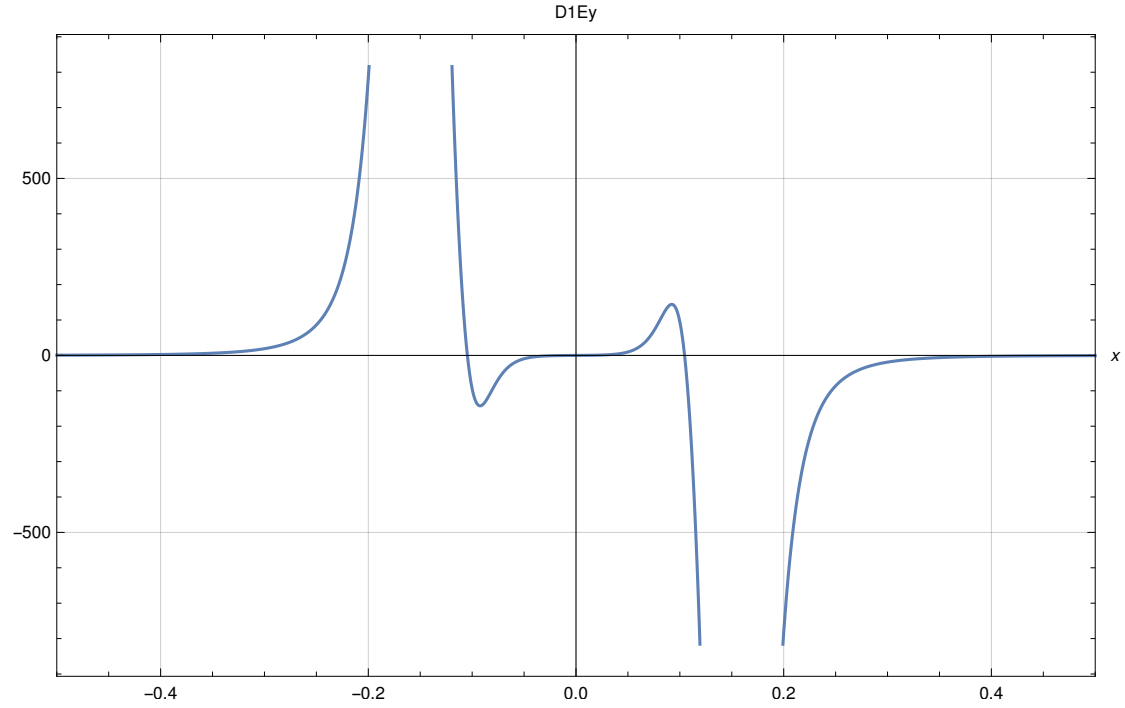

Out[30]=

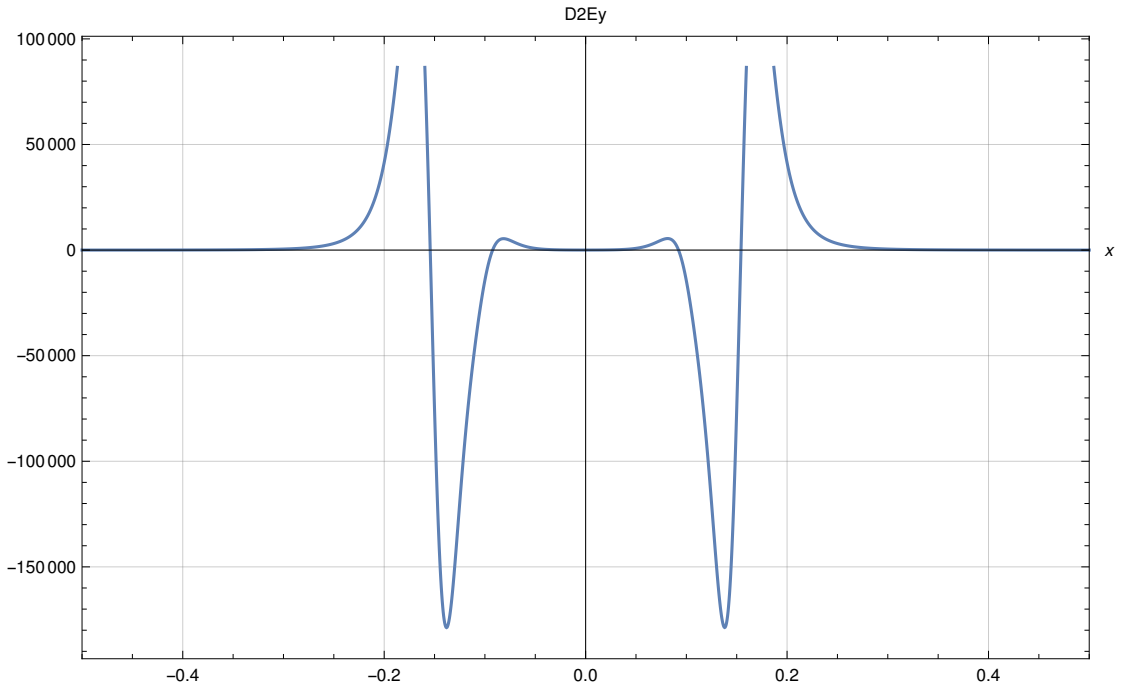
D2Ey
100 000
50 000
0
−50 000
−100 000
−150 000
−0.4
−0.2
0.0
0.2
0.4
x

Out[31]=

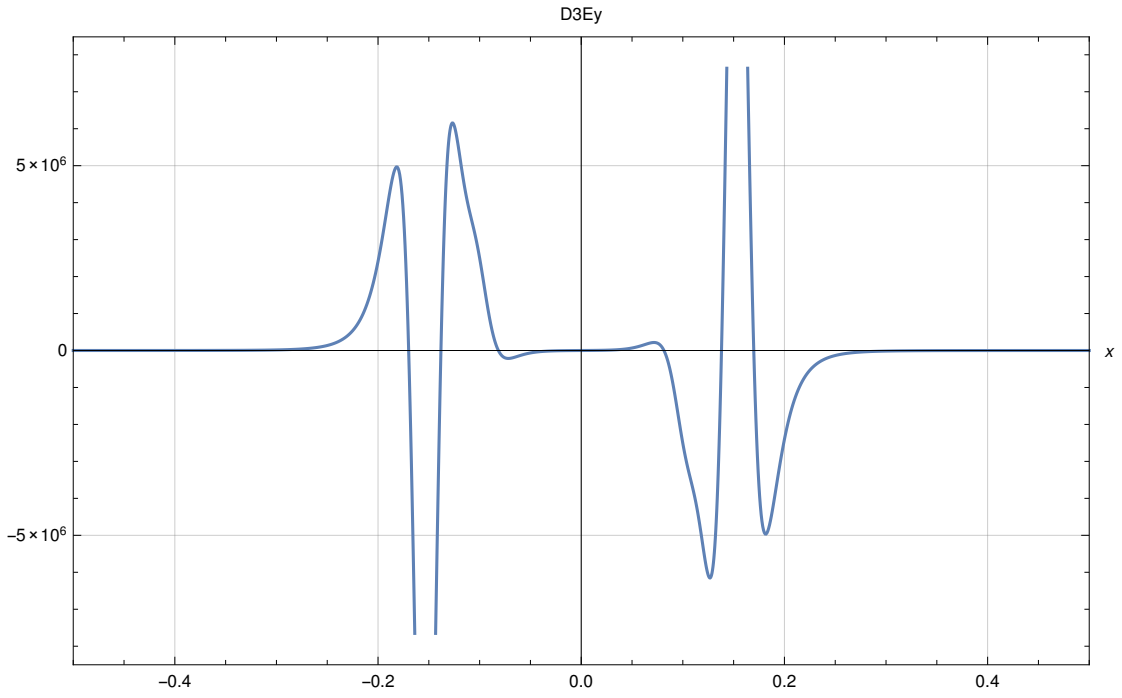
D3Ey
5 × 10^6
0
−5 × 10^6
−0.4
−0.2
0.0
0.2
0.4
x

Out[32]=